JOURNAL OF CATALYSIS 95, 587–601 (1985)

Effect of Varying Titania Surface Coverage on the Chemisorptive Behavior of Nickel

G. B. RAUPP[1] AND J. A. DUMESIC[2]

Department of Chemical Engineering, University of Wisconsin, Madison, Wisconsin 53706

Received March 2, 1985; revised June 3, 1985

Temperature-programmed desorption (TPD) of CO and H_2 from nickel surfaces containing varying amounts of titania showed that the effects of titania adspecies are predominantly short-ranged. Titania surface species block CO adsorption at strongly bound sites (believed to be sites atop individual Ni atoms) corresponding to heats of adsorption in the range 134–139 kJ · mol^{-1}; in addition, titania enhances adsorption into more weakly bound sites (believed to be bridging and hollow sites between Ni atoms) with heats of adsorption from 91 to 107 kJ · mol^{-1}. For hydrogen adsorption, overall adsorption strength was increased with increasing concentration of surface titania. In addition, a new, activated adsorption state was created and is believed to be associated with hydrogen at sites on titania. The variations of the initial sticking coefficients of CO and H_2 as a function of titania precoverages show that at low titania coverage each TiO_x moiety influences approximately 4–10 Ni surface atoms. The long-range electronic influence of titania at a concentration of 0.1 monolayer was estimated to be responsible for only a 6-kJ · mol^{-1} decrease in the CO heat of adsorption. Qualitatively, similar results were found for an alumina-containing Ni surface, although alumina appears to be more poorly dispersed than titania on Ni. This suggests that the effects of metal oxide species on metal surfaces may be generalized to include irreducible support materials.

INTRODUCTION

In a previous study of temperature-programmed desorption of CO and H_2 from a titania-containing polycrystalline nickel surface (*1*), we showed that the presence of titania species on metal surfaces may be responsible for CO and H_2 chemisorption behavior typically observed for catalysts exhibiting so-called strong metal–support interactions. Specifically, titania adspecies on a polycrystalline nickel foil blocked CO adsorption sites and weakened CO adsorption strength. Hydrogen adsorption into sites typical of clean nickel was suppressed in favor of a more strongly bound, activated adsorption state. These results strongly suggested that titania moieties migrate onto the surfaces of supported metal particles during high-temperature reduction. In addition, Kugler and Garten (*2*) patented an unsupported nickel catalyst promoted with titania and demonstrated that it exhibits CO hydrogen behavior typical of titania-supported nickel catalysts. Analogous results were reported by Sudhakar and Vannice (*3*) for titania-promoted Pt. Chung *et al.* (*4*) have further demonstrated the promotional properties of submonolayer amounts of titania on Ni(111) for methanation. In this paper we present an investigation of the effects of titania surface coverage on the chemisorptive behavior of CO and H_2 on nickel. Varying the titania coverage not only allowed a determination of the extent of long-range versus short-range influences of the titania, but also provided an estimate of the titania coverage required to observe significant alterations of the chemisorptive properties of nickel surfaces.

The effects of oxygen and carbon as well as alumina surface additives are presented. The purpose of the experiments with oxygen and carbon was twofold. First, the

[1] Present address: Department of Chemical and Bio-Engineering, Arizona State University, Tempe, Ariz. 85287.

[2] To whom correspondence should be addressed.

0021-9517/85 $3.00

results allowed us to rule out the presence of carbon and/or oxygen contamination as a cause of the chemical effects attributed to titania which were inferred from the CO and H_2 thermal desorption measurements. Second, the effects of these adatoms could be directly compared to the effect of titania surface species to provide additional information about the nature of the adlayer–substrate interactions. The effects of alumina adspecies on nickel were studied to address the question of how general are the effects of metal oxide species on metal surfaces for support materials other than transition metal oxides such as titania. Alumina was chosen as the test material because it is a common commercial support, and because it is much less reducible than titania.

EXPERIMENTAL

Temperature-programmed desorption (TPD) experiments were performed in the UHV chamber as described previously (*1*). Titanium powder (Alfa, 99.98%) was evaporated *in situ* from a boron nitride crucible held at 1773 K as measured with a tungsten–rhenium thermocouple with the evaporator in direct line of sight with the sample. Typical deposition rates were 0.025 nm $\cdot$ s^{-1}. A rotary feedthrough shutter and calibrated quartz crystal thickness monitor were used to achieve controlled amounts of titanium on the nickel surface. The thickness monitor was calibrated assuming a nominal density for the evaporated titanium layer of 4.5 g $\cdot$ cm^{-3}. Assuming a contiguous overlayer of Ti, the thickness of the evaporated layer was independently estimated from the attenuation of the Ni $2p_{3/2}$ XPS peak intensity, assuming the emitted photoelectron mean free path to be 1.28 nm. This calculation agreed to within 20% of the value estimated with the thickness monitor.

The sample was held at 300 K during deposition, during which time the background pressure increased to 8×10^{-7} Pa and consisted principally of H_2, CO, and H_2O. Following deposition the surface was exposed to $^{18}O_2$ at 300 K to oxidize the titanium and nickel, followed by H_2 exposure from 300 to 150 K (while cooling the sample) and subsequent flashing to 620 K to reduce the nickel. Alternatively, the titanium was oxidized through exposure to D_2O at room temperature or below, followed by flashing to 620 K. It was found that D_2O dissociates on reduced titania (D_2 is desorbed) leaving oxygen atoms on the surface which oxidize the titanium (*5*). Deuterated water was dosed and the surface flashed in succession until D_2 desorption could not be detected (this never required more than 3 dose/flash cycles). Surfaces prepared by either $^{18}O_2$ or D_2O oxidation behaved identically with regard to subsequent CO and H_2 desorption.

The polycrystalline Ni foil (Alfa, 99.998%; 2 cm diam. and 0.127 mm thick) was initially cleaned prior to titania deposition by repeated cycles of low-pressure oxidation (ca. 10^{-4} Pa $\cdot$ s at 300 K) followed by high-temperature annealing (973 K, 30 min) and argon ion sputtering (3 kV, 25 mA, 30 min). A final high-temperature vacuum treatment of 40 min duration was necessary to remove surface defects caused by the ion bombardment. This procedure has been shown to remove all surface contaminants except ca. 2% of a monolayer of C from Ni single crystals (*6*).

Fractional titania coverages, in terms of monolayer equivalents, are quoted as the number of titanium atoms deposited divided by the assumed monolayer site density of the nickel foil (mean of (111) and (100) planes = 1.74×10^{19} atoms Ni $\cdot$ m^{-2} = 1 monolayer = 1 ML). The oxidation state of the titania adlayer is unknown due to the lack of *in situ* surface analysis. It is believed that the titania is not fully oxidized; accordingly, titania is denoted as TiO_x, with $x < 2$. Chung *et al.* (*4*) have prepared titania adlayers on Ni(111) and determined that x ranged from 1.0 to 1.5 based on Auger electron spectroscopy measurements. Prior to each deposition of titanium the surface was cleaned with 3–4 extended cycles of argon ion bombardment and high-tem-

perature annealing. Reattainment of surface cleanliness was verified through the CO desorption measurements.

The precleaned Ni polycrystalline foil was carburized by cracking ethylene (Matheson, 99.5%). Ethylene adsorbed at 150 K decomposed upon flashing to 600 K, liberating hydrogen and leaving C on the surface. LEED and Auger analyses of similarly treated Ni single-crystal surfaces have shown that surface carbides are formed that are stable under UHV conditions below 600 K (*7, 8*). Above 600 K a fraction of C may diffuse into the bulk; above 700 K the carbide is transformed to graphitic carbon. The amount of surface carbide was estimated from the absolute amount of hydrogen liberated upon flashing the ethylene-exposed surface, with correction made for background hydrogen adsorption.

Aluminum rod (99.999%, Alfa) was evaporated *in situ* onto the precleaned nickel foil maintained at ca. 250 K from an alumina crucible held at 1320 K. The deposition rate was ca. 0.05 nm · s^{-1} as measured with the calibrated quartz crystal thickness monitor. During deposition the chamber background pressure increased to 2×10^{-7} Pa. The sample was subsequently exposed to $^{18}O_2$ at 300 K to oxidize Al metal, then exposed to H_2 at 150 K and flashed to reduce the Ni. In this study only one alumina coverage (ca. 1.2×10^{19} atoms Al · m^{-2}, $\theta_{Al} = 0.7$ ML equivalent) was investigated.

RESULTS

Carbon Monoxide Desorption from TiO_x/Ni

The influence of different coverages of predeposited TiO_x on CO thermal desorption is shown in Fig. 1. The TPD traces represent desorption from saturated CO surfaces; this required larger CO exposures with increasing TiO_x coverage since titania decreased the sticking coefficient for CO adsorption. For the clean Ni surface, CO desorbs in first-order fashion near 460 K; this adsorption state is denoted as α_1(Ni).

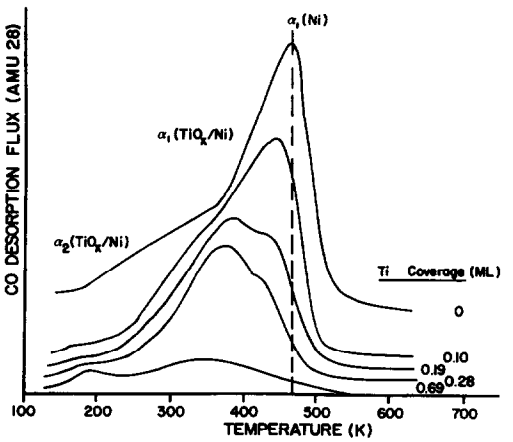

FIG. 1. Effect of varying TiO_x precoverage on CO thermal desorption from Ni. CO coverage at saturation.

The low-temperature shoulder at ca. 250–350 K is indicative of weaker adsorption sites, denoted as α_2(Ni), which filled only after the α_1(Ni) states neared saturation.

The desorption activation energy for the α_1 peak was estimated to be 134 kJ · mol^{-1} at saturation coverage, assuming first-order desorption kinetics and a preexponential factor of 10^{16} s^{-1}, a value typically measured for Ni single crystals (*6, 9, 10*). Similar values were estimated using the heating rate variation method (*9*), in which no assumptions concerning desorption order or preexponential need be made.

A small amount of TiO_x ($\theta_{Ti} \sim 0.1$ monolayer equivalent) significantly decreases the saturation CO coverage of the α_1 state. Inhibition of CO desorption characteristic of clean Ni is accompanied by filling of states at lower temperatures (i.e., enhanced desorption in the range 300–400 K), characteristic of TiO_x-perturbed Ni sites. These states are denoted as α_1(TiO_x/Ni). It is important to note that this behavior is indicative of a relatively short-ranged effect of tiania on CO adsorption, as opposed to the continuous gradual downward shift in peak temperature which would only be observed with increasing TiO_x coverages for long-range interactions.

New states are also observed at 200 K.

Experiments on an oxidized titanium foil showed that the low-temperature peak is due to CO adsorption directly on the titania (*11*), and these are denoted as $\alpha_2(TiO_x/Ni)$. Saturation coverages for CO on titania were found to be low, and were estimated to be in the range of 0.01–0.08 of a monolayer, consistent with the small peaks presently observed for the titania-containing surfaces.

A small but significant shift equal to 20 K for the Ni α_1 state is evident upon the first addition of a small amount of titania. Such shifts have not been observed for Cl and P overlayers on single-crystal Ni (*12*), but have been observed for small precoverages of sulfur (*12, 13*).

No second-order CO desorption peaks were observed, suggesting that adsorbed CO does not readily dissociate on the titania-containing Ni surfaces under UHV conditions. It cannot be discounted, however, that a fraction of adsorbed CO dissociates and does not desorb below the maximum temperature of the TPD experiments.

Carbon Monoxide Desorption from Carbided Ni

Figure 2 shows the effect of varying carbidic carbon coverage from 0 to 0.75 ML on the CO TPD traces from near saturation (ca. 90%) coverage. This CO coverage was obtained by exposure of the sample to 5 L (Langmuirs) of CO at 150 K (1 L = 1.3×10^{-4} Pa · s). As for TiO_x, addition of C adatoms results in a monotonic conversion of CO desorption from sites characteristic of clean Ni to desorption from sites characteristic of surface-carbided Ni. The effect of carbidic carbon on the binding energy of CO is similar to the effect of titania. Indeed, the desorption activation energy for the α NiC state was estimated to be 91 kJ · mol^{-1} (assuming first-order desorption and a preexponential of 10^{13} s^{-1}), the same estimate for the average energy for the $\alpha_1(TiO_x/Ni)$ state. This value is in the range of energies reported for carbided nickel single crystals (*7, 8*).

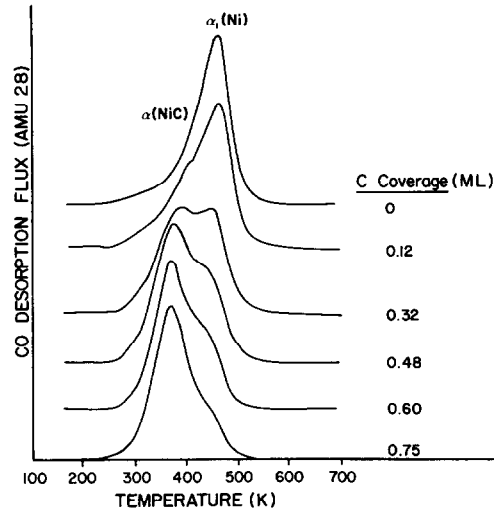

FIG. 2. Effect of varying C coverage on CO thermal desorption from Ni. CO exposure was 5 L (Langmuirs) at 150 K.

Carbon monoxide adsorption behavior on carbided Ni differs significantly in several ways from that on titania-containing Ni. First, no measurable shift in the Ni α_1 peak temperature was detected at low C coverages. Second, titania surface species cause a noticeably broader distribution of adsorption sites than does C as seen by the respective desorption peak half-widths of 200 and 90 K. Finally, saturation CO coverages are dramatically different. Figure 3 compares the dependence of total CO coverage and the amount of CO adsorbed in the Ni α_1 state versus adlayer precoverages for the two types of surfaces. The amount of CO adsorbed in the Ni α_1 state was estimated by resolving the TPD curve assuming first-order desorption kinetics. Note that CO exposure for the series of carbided Ni desorptions was constant at 5 L. This was sufficient to achieve ca. 90% of total saturation coverage and complete saturation of the Ni α_1 state. The upper plot shows that carbidic carbon does not block total CO adsorption, in contrast to TiO_x which blocks a significant number of CO adsorption sites. The effect of TiO_x on the Ni a_1 state population is somewhat more

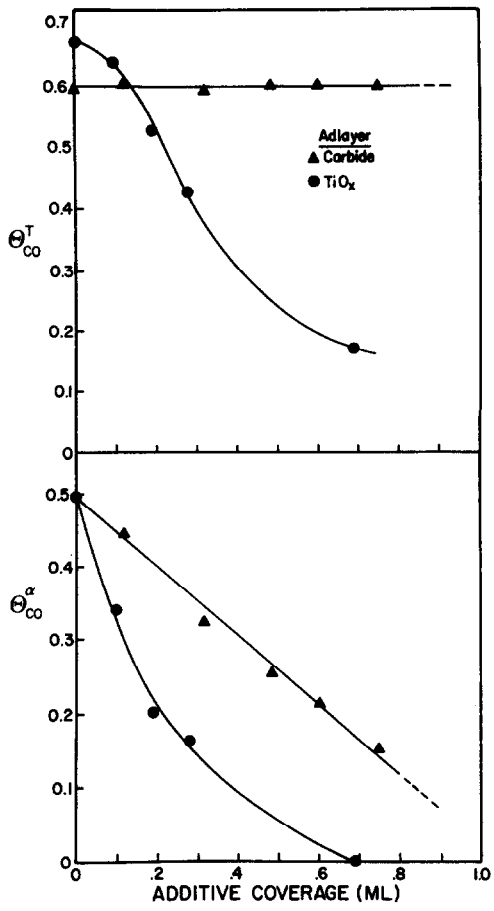

FIG. 3. Dependence of total CO coverage, θ^T_{CO}, and α_1-state coverage, θ^α_{CO}, on additive coverage.

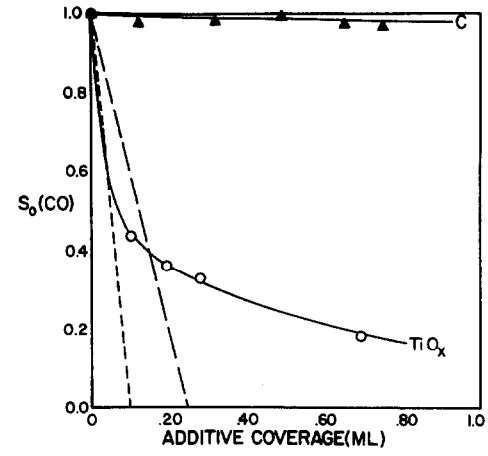

FIG. 4. Variation of the initial sticking coefficient of CO, S_0, as a function of additive coverage. S_0 evaluated at 150 K. Long dashed line represents the theoretical dependence according to the relationship S_0 proportional to $(1 - 4\theta_{Ti})$; short dashed line represents S_0 proportional to $(1 - 10\theta_{Ti})$.

pronounced than C, the latter causing an approximately one-to-one decrease in CO molecules adsorbed in this state per surface C atom.

From a series of TPD runs of varying CO exposure, plots were constructed of CO coverage versus CO exposure for each of the TiO_x and C precoverages under investigation. Initial sticking coefficients (S_0) were estimated from the initial slopes of these plots, assuming a value of $\theta^T_{CO} = 0.67$ ML at saturation for the clean Ni surface (*14, 15*). As shown in Fig. 4, the initial sticking coefficient for CO strongly depends on the TiO_x coverage but is nearly independent of the C coverage.

Carbon Monoxide Desorption from Oxidized Nickel

The effect of extent of nickel oxidation on CO adsorption/desorption behavior is shown in Fig. 5. For low oxygen preexposures at 300 K the Ni α_1 state population decreases while population in weaker states desorbing from 150 to 350 K increases. Unlike C or TiO_x, the presence of nickel oxide

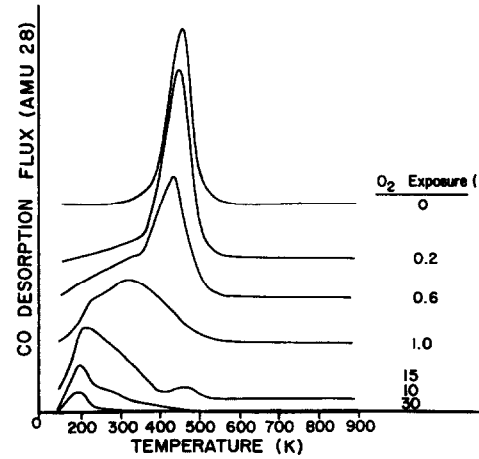

FIG. 5. Effect of varying oxygen preexposure on CO thermal desorption from Ni. CO exposure was 3 L at 150 K.

does not give new adsorption states of constant peak temperature, or average desorption energy, with increasing oxygen coverage. Instead, a continuous decrease in average adsorption strength is observed as the surface becomes more oxidized. In large part this behavior can be attributed to oxidic layer formation at larger oxygen exposures; note that, unlike oxygen, the carbon and titania "adlayers" are restricted to the surface.

Carbon Monoxide Desorption from Al_2O_3/Ni

The effect of a high coverage of surface alumina (i.e., $\theta_{Al} \sim 0.7$ monolayer equivalent) on nickel with respect to carbon monoxide thermal desorption can be seen graphically in Fig. 6. In the upper portion of the figure (labeled A), it is evident that the majority of the adsorbed carbon monoxide desorbs via a first-order process (indicative of molecular adsorption) in a manner not significantly different than desorption from clean nickel. The lower portion of the figure (labeled B) compares desorption from saturation CO coverages on clean Ni and the alumina-containing surface. The effect of surface alumina is twofold. First, alumina blocks a small number of the most strongly bound, or α_1, states as shown by the decrease in peak intensity at the highest desorption temperatures. Site blocking is accompanied by chemical modification. This is evident in comparing the α_1 peak temperatures at saturation of 450 and 435 K for the clean and alumina-containing surfaces, respectively. New sites are also apparently created corresponding to enhanced desorption in the range 300–400 K from the Al_2O_3/nickel surface.

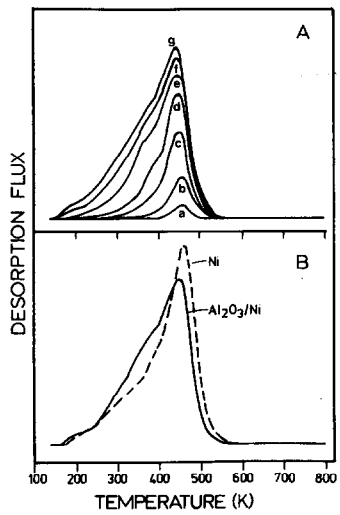

FIG. 6. (A) CO desorption from Al_2O_3/Ni following different CO exposures at 150 K; (a) 0.1, (b) 0.4, (c) 1.0, (d) 1.8, (e) 3.2, (f) 8.0, and (g) 20 L. (B) CO desorption from saturation coverage at 150 K on (h) clean Ni and (i) Al_2O_3/Ni. Alumina coverage was 0.7 ML.

Using the heating rate variation method, the CO adsorption strength (desorption activation energy) was found to be decreased by the presence of Al_2O_3 adspecies from 135 kJ · mol^{-1} ($\nu = 8 \times 10^{15}$ s^{-1}) on the clean surface to 128 kJ · mol^{-1} ($\nu = 3 \times 10^{15}$ s^{-1}). Since the new states created by alumina were only present as a shoulder in the TPD spectra, the heating rate method could not be employed to estimate adsorption strengths of these new weaker states. Assuming first-order desorption kinetics, these states can be estimated to be in the range 80–93 kJ · mol^{-1} (for a preexponential of 10^{13} s^{-1}).

Saturation CO coverage including all adsorbed states was 86% of saturation coverage on the clean nickel surface. The initial sticking coefficient for the α_1 state remained high in spite of the presence of surface alumina, and was estimated to be ca. 0.9.

Hydrogen Desorption from TiO_x/Ni

Adsorption–desorption behavior of H_2 was also studied on the nickel surface with varying TiO_x coverage. For adsorption at 150 K, hydrogen thermal desorption spectra from the respective saturation coverages are compared in Fig. 7. The TPD traces reveal a continuous decrease in the population of the β_1 and β_2 adsorption states characteristic of clean Ni as titania coverage increases. New states are apparently simultaneously created, giving rise to

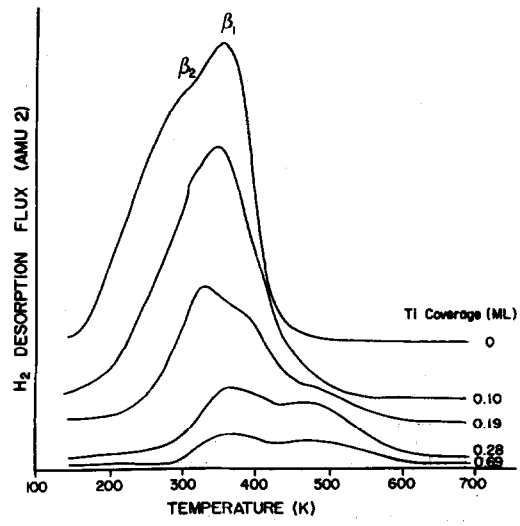

FIG. 7. Effect of varying TiO_x coverage on H_2 thermal desorption from Ni following saturation H_2 exposure at 150 K.

desorption peaks at ca. 360 and 480 K. The population of the strongest state (desorption temperature ca. 480 K) appears to go through a maximum at a TiO_x coverage of 4.2×10^{18} Ti atoms/m^2 (θ_{Ti} = 0.28 monolayer equivalent). Because desorption of each observed state is described by recombination of hydrogen atoms, second-order desorption kinetics apply and cause upward shifts in peak temperatures with decreasing initial adsorbate coverage. A portion of the observed upward shift in peak temperatures is due, therefore, to initial hydrogen coverage differences; the remainder is due to an increase in hydrogen adsorption strength. Assuming a preexponential of 10^{-6} $m^2 \cdot$ molecules$^{-1} \cdot s^{-1}$, a value typical for second-order desorption, estimated desorption activation energies increased from 86 and 66 kJ $\cdot$ mol^{-1} for the β_1 and β_2 states, respectively, on the clean surface to 108 and 75 kJ $\cdot$ mol^{-1} for the high- and low-temperature states, respectively, on the 0.69-ML TiO_x/Ni surface.

Figure 8 graphically illustrates the variation in total H_2 uptake and initial H_2 sticking coefficient evaluated at 150 K as a function of TiO_x coverage. Through comparison with Figs. 3 and 4, it can be seen that the effect of TiO_x is more severe for H_2 than CO in terms of the observed reduction in total saturation coverage and initial sticking coefficient for a given titania surface concentration. For example, titania coverage θ_{Ti} = 0.28 monolayer equivalent reduces the total hydrogen coverage, θ_H, by a factor of 3 and S_0 (H_2) by nearly two orders of magnitude, compared to reduction of θ_{CO}^T by only ca. 35% and S_0 (CO) by a factor of 3.

As observed previously (*1*), increasing the surface temperature during hydrogen exposure to 300 K allowed more hydrogen to be adsorbed into a higher temperature, activated state, which desorbed above 500 K. Inclusion of the population of this state into the total hydrogen coverage revealed that θ_H remained invariant (to within −20%) as increasing amounts of titania were deposited on the nickel surface.

Hydrogen Desorption from Al_2O_3/Ni

Following hydrogen exposure at 150 K, H_2 desorbs from the alumina-containing nickel surface from at least two adsorption

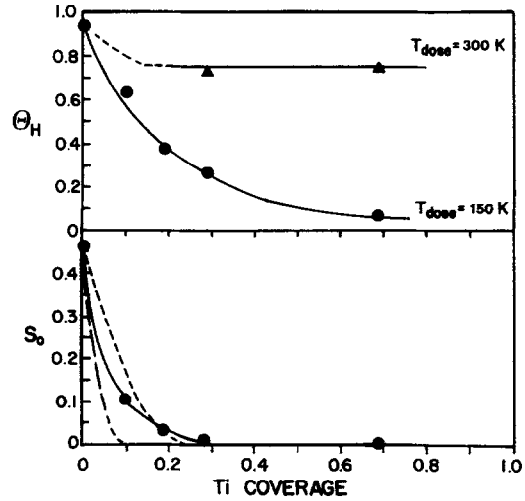

FIG. 8. Variation of total H_2 coverage, θ_H, and initial sticking coefficient of H_2 as a function of titania coverage. S_0 evaluated at 150 K. Short dashed line represents the dependence S_0 proportional to $(1 - 4\theta_{Ti})^2$; long dashed line represents S_0 proportional to $(1 - 10\theta_{Ti})^2$.

states as shown in Fig. 9A. These partially overlapping desorption peaks are due to recombination of atomic hydrogen as confirmed by isotopic mixing experiments.

Figure 9B compares desorption following saturation H_2 coverage for the Ni and Al_2O_3/Ni surfaces. It can be seen that the two major adsorption states observed on Al_2O_3/Ni following exposure at 150 K apparently correspond to the β_1 and β_2 states desorbed from clean nickel; the presence of surface Al_2O_3 preferentially blocks the most strongly bound, or β_1, state. In addition, a third adsorption state, or distribution of states, is created as evidenced by increased desorption in the 400–500 K range. This third state with a higher desorption activation energy than the β_1 or β_2 states became more apparent following large exposures (ca. 10,000 L) at 300 K (see curve (i) in the figure). This increase in adsorption extent as the surface temperature during H_2 exposure is increased is evidence for an activation energy barrier for adsorption into the strongest adsorption state.

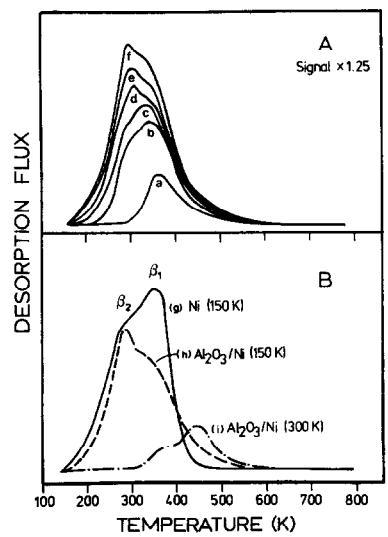

FIG. 9. (A) H_2 desorption from Al_2O_3/Ni following different H_2 exposures at 150 K: (a) 0.3, (b) 1.0, (c) 3.0, (d) 5.0, (e) 13, and (f) 30 L. Alumina coverage was 0.7 ML. (B) H_2 desorption from saturation coverage on (g) clean Ni dosed at 150 K, (h) Al_2O_3/Ni dosed at 150 K, and (i) Al_2O_3/Ni dosed at 300 K.

For an adsorption temperature of 150 K, the "saturation" coverage of hydrogen was 74% of the clean nickel saturation coverage. Taking into account the additional adsorption capacity in the high-temperature range achieved through exposures at higher temperatures, saturation coverage was 78% of the clean nickel value.

DISCUSSION

The Role of Titania Adspecies

The effect of electronegative or electropositive surface additives on CO and H_2 chemisorption on Ni has previously been attributed to changes in the electron density of the surface Ni layer (*12, 16–18*). In contrast, Madix and co-workers (*13, 19, 20*) have reported that the interference of CO adsorption on Ni(100) by sulfur adatoms can be explained by simple site blocking. In order to understand these interpretations, it is useful to review the commonly accepted model for CO and H_2 bonding to a Group VIII metal surface.

Carbon monoxide–Group VIII metal bonding is described with the Blyholder model (*21, 22*). The chemisorptive bond is formed through the C atom in a donor–acceptor mechanism as follows: occupied 5σ CO orbitals donate electrons to the metal *d*-electron orbitals which, in turn, back-donate charge to the antibonding $2\pi^*$ CO orbitals, effectively weakening the C–O π bond. The reduced CO adsorption bond strength and adsorption rate on Ni(100) in the presence of electronegative adatoms S, Cl, and P has been attributed to reduced Ni 3*d* electron density and a corresponding decrease in the extent of electron back-donation (*12–18*) or to physical site blocking (*13, 19, 20*). In contrast, the presence of electropositive adatoms, K, Na, and Cs was observed to increase CO adsorption strength and dissociation rate; this was attributed to increased Ni 3*d* electron density (*17*).

The adsorption character of hydrogen on Ni is less well-defined. Terminal and bridge-bonded forms may exist on single

crystal surfaces, with bridge-bonded forms favored in the presence of coadsorbates (*23*). In attempting to predict the effects of adatoms on hydrogen chemisorption relative to CO adsorption, it is important to note both that the charge transfer from Ni to H required to form the Ni–H bond is less than that required from Ni to CO (*24*), and that two neighboring surface sites are necessary for dissociative H_2 adsorption.

The present results confirm that the influence of titania surface species on the chemical nature of nickel CO and H_2 adsorption sites is relatively short-ranged. Consider first carbon monoxide chemisorption. The presence of TiO_x weakens the CO–nickel bond strength to a degree similar to chlorine (*12*), carbidic carbon, and surface oxygen. This observation is consistent with the conclusion of Santos *et al.* (*25*), who suggested alteration of the kinetic behavior of Fe/TiO_2 ammonia synthesis catalysts was due to the presence of *electronegative* TiO_x species on the surface of the iron particles. Unlike carbidic carbon, but similar to chlorine, sulfur, and phosphorous, TiO_x was also observed to block a fraction of the Ni adsorption sites. Of importance for the present discussion is how many Ni surface atoms each TiO_x moiety modifies or blocks.

Examination of the modification of CO–Ni bonding as a function of TiO_x concentration allows differentiation between short- and long-range interactions. In the extreme, if only local interactions are important, new binding states will be observed near the modifier only, while the remainder of the surface sites are unperturbed. If long-range interactions dominate, incremental addition of adspecies will affect all adsorption sites.

It is clear that an individual TiO_x moiety modifies a limited number of Ni adsorption sites. As TiO_x concentration was increased, a smooth replacement of clean surface states characteristic of the modified surface was observed. The plots in Figs. 3 and 4 provide a measure of the effective interaction range. The influence of titania is most pronounced with respect to the decrease in the clean Ni α_1 state population. The lower plot in Fig. 3 shows the range of this effect to be of the order or slightly greater than the nearest-neighbor nickel atoms. From the initial slope of the plot of initial CO sticking coefficient versus titania coverage in Fig. 4, it appears that at low coverage 1 TiO_x affects approximately 6 Ni adsorption sites. Allowing for an error in absolute TiO_x coverage of ±40%, this value can be bracketed such that each TiO_x affects not less than 4 and not more than approximately 10 Ni surface atoms (note that theoretical curves S_0 proportional to $[1 - 4\theta_{Ti}]$ and $[1 - 10\theta_{Ti}]$ are included in the figure). At higher coverages increased tendency toward clustering of the adlayer species probably takes place and results in a smaller number of Ni sites being perturbed per incremental TiO_x surface coverage; similar behavior has been observed by Kiskinova and Goodman for phosphorus overlayers on Ni(100) (*17*). Note that the relatively short interaction range estimated above coupled with the observation that the Ni α_1 site is completely blocked at a titania coverage of 1.0×10^{19} atoms Ti $\cdot$ m^{-2} ($\theta_{Ti} = 0.69$) allows us to conclude that the titania is relatively well dispersed over the Ni surface.

Because of the errors inherent in determining absolute surface coverages, the exact nature of the mode by which TiO_x locally alters CO adsorption sites on Ni cannot be deduced. In general, the surface structure of the overlayer, in addition to atomic size, electronegativity, and "adsorption" site of the adlayer species, must be considered to make such deductions. For example, on the basis of LEED patterns, it was determined that S and Cl adatoms have four nearest-neighbor nickel atoms on a Ni(100) surface (*12*). Since the initial sticking coefficient for CO adsorption into the most strongly bound clean Ni state at low S and Cl decreased at a rate faster than that predicted by the simple site blocking model, or sticking coefficient proportional to $(1 - 4\theta_{S \text{ or } Cl})$, it was concluded that

S and Cl adatoms exhibit long-range (greater than first nearest neighbor) electronic interaction with the Ni surface. At low adatom coverage, a small shift in the high-temperature CO desorption state was also taken as evidence of electronic interaction.

In the present study, a titania coverage of $\theta_{Ti} = 0.1$ shifted the α_1-CO peak ca. 20 K relative to the clean Ni surface. This small shift shows the long-range electronic effect of titania at this coverage on the binding energy of CO on Ni is no greater than about 6 kJ · mol^{-1}. A similar upper limit has been estimated for sulfur adatoms (*20*). The new adsorption states created upon the addition of titania must, therefore, be due to local effects of the adspecies.

As demonstrated in recent HREELS and TPD studies of CO adsorbed on sulfided Ni(100), much of this local interaction may be explained by geometry or simple site blocking (*13, 20*). A schematic diagram of a clean Ni(100) surface and Ni(100) surfaces containing p(2 × 2)S and c(2 × 2)S overlayers are shown in Fig. 10. Carbon monoxide adsorption on clean Ni (Fig. 10A) occurs linearly on a single Ni (or atop site) up to a coverage of $\theta_{CO} = 0.5$ (*20, 26*). Above this coverage so-called "compression" (*14*) or "domain" structures (*27, 28*) form, with further CO adsorption occurring at bridging sites. The presence of 0.25 ML S completely blocks all atop sites, and subsequent adsorption occurs at bridging or fourfold hollow sites (Fig. 10B). Half-monolayer S precoverage (Fig. 10C) allows CO adsorption into a fourfold hollow site surrounded by four sulfur atoms. Note that the presence of S adatoms causes CO to adsorb at sites *that would not otherwise be occupied* at high coverage due to CO–CO repulsive interactions.

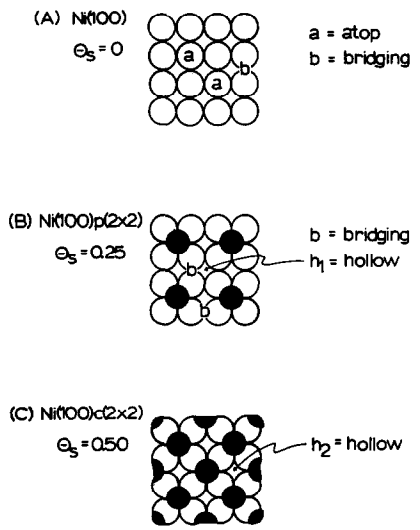

FIG. 10. Schematic of adsorption sites on (A) clean and (B, C) sulfur-covered Ni(100) (adapted from (*20*)).

HREELS combined with temperature-interrupted thermal desorption allowed Gland *et al.* (*20*) to assign each of these sites to characteristic CO desorption peak temperatures, as reproduced in Table 1. The similarity of the present CO TPD results with those of Gland *et al.* suggests that dispersed titania adspecies block CO adsorption on strongly held, linear atop sites and allow adsorption onto less strongly bound hollow or bridging sites. Moreover, this interpretation is supported by the recent work of Takatani and Chung (*29*) on a nickel film deposited on titania. Following extended high-temperature reduction during which time titania migrated onto the nickel surface, HREELS measurements showed no CO stretching bands near 2050 cm^{-1} (atop sites) nor near 1920 cm^{-1} (bridging sites). Instead, only a band at 1850 cm^{-1} was observed, which was assigned to "a site near the surface titanium oxide on nickel." This stretching frequency is similar to the peak at 1815–1845 cm^{-1} observed on Ni(111) attributed to a threefold site (*30*) (note that there are no fourfold hollow sites on Ni(111)). The lack of precise structural characterization of the surface studied presently precludes unambiguous site assignment. Nonetheless, on the basis of the literature discussed above, we suggest that the effect of surface titania with respect to CO adsorption is relatively short-ranged, and can largely be explained in geometric terms. Electronic effects, although present,

TABLE 1

Assignment of CO Adsorption Sites to CO Desorption Temperatures for Ni(100) and Ni(100) Sulfur-Modified Surfaces[a]

Binding site	Designation	Desorption temperature (K)	CO stretching frequency (cm^{-1})
Onefold atop terminal site on clean Ni(100)	a	425	2050
Twofold Ni bridge on clean Ni(100)	b	290	1960
Twofold Ni bridge site on Ni(100) p(2 × 2)S	b	290	1910–1960
Fourfold Ni hollow on Ni(100) p(2 × 2)S	h_1	370	1740
Fourfold Ni hollow on Ni(100) c(2 × 2)S	h_2	140–150	2115

[a] Results from Gland *et al.* (*20*).

are apparently of secondary importance. This means that for large supported Ni crystallites, TiO_x surface species *must* be present for these crystallites to exhibit the chemisorption behavior indicative of so-called strong metal–support interactions.

The differences observed between CO desorption from the oxygen-exposed Ni surface and the TiO_x-containing or carbided Ni surfaces can largely be attributed to oxidic layer formation at higher oxygen exposures. The sticking probability of oxygen on nickel surfaces is high (ca. 0.8) up to one-half monolayer coverage but falls by at least an order of magnitude after this point as oxide layer formation begins (*31*). Thus, for appropriate comparisons of the effects of surface oxygen, TPD traces following O_2 preexposures less than about 1 L will give a surface containing oxygen adatoms without subsurface oxygen influences or nickel lattice distortions (*32, 33*). A low levels of oxygen surface coverage the weakening of the CO–Ni chemisorption bond strength is in the same range as the weakening due to TiO_x or carbidic carbon. Carbon monoxide adsorption strength is further weakened as subsurface oxygen is incorporated into the distorted metallic nickel lattice.

Quantitative differences between Ni surfaces containing C adatom and TiO_x adspecies can most likely be explained in steric terms, as a carbidic carbon atom is smaller than an oxidic moiety.

Results for hydrogen adsorption, while being less definitive than the results for CO adsorption, are consistent with a short-range influence of titania on nickel. At low TiO_x coverage the initial sticking coefficient for hydrogen adsorption decreases according to S_0 proportional to $(1 - 4\theta_{Ti})^2$ or $(1 - 10\theta_{Ti})^2$; note that the effect of adspecies on hydrogen is greater than for CO since H_2 requires two adjacent Ni sites for dissociative adsorption. Of particular interest is the observation that TiO_x increases the overall strength of hydrogen adsorption, in contrast to electronegative adatoms such as C, S, Cl, or P which decrease H_2 adsorption strength. It appears that the effects of titania cannot be described in simple electronic terms; instead other factors must be controlling. On clean or titania-containing Ni surfaces, H adatoms most likely adsorb at bridging or hollow sites, and thus titania does not necessarily create new sites on the nickel. The observed increased binding energy could be a consequence of direct bonding of hydrogen adatoms to the oxygens associated with surface titania, or of a steric hindrance to hydrogen adatom migration and recombination, prerequisite steps for molecular H_2 desorption.

The impact of these changes in the binding sites and adsorption strengths of surface reactants on CO hydrogen behavior will be discussed in a later publication.

The Role of Alumina Adspecies

There exists considerable evidence in the literature that supports such as alumina and silica can exert measurable influences on the catalytic behavior of supported metal particles. For example, the CO hydrogenation activity of Group VIII metals is approximately one order of magnitude higher when supported on alumina as compared to silica (*34–36*). High-temperature reduction significantly reduces *n*-pentane or *n*-hexane hydrogenolysis activity over Pt/Al_2O_3 (*37*). Air oxidation restores catalytic activity and hydrogen chemisorption. Dautzenberg and co-workers (*38, 39*) have observed similar behavior for the same system. Platinum on silica also exhibits suppression of hydrogen chemisorption after reduction above 970 K, which again could be partially reversed by treatment in oxygen (*40*). For nickel supported on silica, high-temperature reduction resulted in a slight increase in CO hydrogenation activity but a one order of magnitude decrease in ethane hydrogenolysis or benzene hydrogenation activities (*41*). This behavior was attributed to NiSi alloy formation during high-temperature reduction (*42*).

Qualitatively, the present results show that an alumina-containing Ni surface exhibits many of the same features as a titania-containing surface with respect to CO and H_2 chemisorption. Both alumina and titania decrease the strength and extent of CO adsorption on nickel. The α_1, or most strongly bound, molecular state is affected most severely. Site-blocking is accompanied by a measurable but small decrease in adsorption strength (desorption activation energy). The surface Al_2O_3 and TiO_x species also convert a portion of this high-temperature state (α_1) to lower temperature states which desorb between 300 and 400 K. Thus, in addition to expected site-blocking, titania as well as alumina decrease the adsorption strength of CO on nickel.

With regard to hydrogen chemisorption, results from alumina- and titania-containing nickel surfaces were also similar. Low-temperature sites are blocked and a new high-temperature state is created. Adsorption into this stronger state is an activated process. The total extent of H_2 chemisorption is not significantly decreased by the presence of titania or alumina when taking into account adsorption into the activated state. The population of the activated state increased with increasing titania adlayer concentration, suggesting that the adsorption sites corresponding to this state are associated with the oxide species. A more specific possibility is that adsorbed hydrogen atoms, originally adsorbed on clean nickel or perturbed nickel sites, diffuse at higher temperatures and "spill over" onto the alumina or titania itself. White and co-workers (*43, 44*) have recently used TPD studies of titania-supported Pt to assign high-temperature adsorption states (desorption temperatures 500–700 K) to spilled-over hydrogen. The greater apparent adsorption strength of these sites may at least be partially due to steric hindrance present in the desorption process which deters surface diffusion and atomic hydrogen recombination. The presence of other adlayer species such as carbon (*8, 45*) or copper (*46, 47*) on nickel has been shown to induce activation energy barriers for hydrogen adsorption. These adspecies also *decrease* the strength of hydrogen adsorption. For high-surface-area titania-supported Rh (*48*) and alumina-supported Pt (*27*), high-temperature reduction created a strongly bound adsorption state as revealed by atmospheric-pressure TPD. These observations further support the contentions that, first, model nickel catalysts containing surface alumina or titania mimic the behavior of corresponding high-surface-area catalysts which have been reduced at high temperatures, and, second, surface alumina and titania modify nickel chemisorptive behavior in a similar way. Thus, an underlying cause of "metal–support interaction" in conventional high-surface-area catalysts, either supported or reducible transition

metal oxides such as titania or on insulating, irreducible oxides such as alumina, may be due to contamination or decoration (*49*) of the surfaces of the metal crystallites by moieties of the support material.

In spite of the apparent similarities between the effects of alumina and titania, several important differences exist. The major difference is the degree to which a similar amount of surface oxidic material modifies the H_2 and CO chemisorption behavior. Surface TiO_x species alter the H_2 and CO adsorption characteristics on nickel to a much greater degree than does alumina at nominally identical concentrations of ca. 0.7 ML equivalent. Comparison of the results for 0.7 ML equivalent alumina with those for varying coverages of titania reveals near equivalent H_2 and CO desorption spectra for a titania coverage of only 0.1 ML equivalent. A similar finding has been reported for S, Cl, and P adlayers on Ni(100), as the effect of P was much less pronounced than either S or Cl (*12*). Since no ordered structure was observed for the P overlayer, in contrast to Cl and S, it was assumed that both a Ni–P surface phase and free Ni coexisted such that a significant number of Ni surface atoms remained unperturbed by P. By analogy, the alumina must exist in a configuration such that a large number of Ni surface atoms remain unperturbed. At a nominally identical titania surface concentration, essentially all Ni surface sites were perturbed. This observation, coupled with the estimate that each TiO_x moiety modified between 4 and 10 Ni surface atoms, suggests that the titania must be relatively well dispersed over the metal surface. In contrast we conclude that alumina is not well dispersed over the Ni but instead exists as discrete, well-separated three-dimensional crystallites. Gorte has reached the same conclusion for alumina adlayers on Pt (*50*). In this configuration only Ni atoms at the periphery of an Al_2O_3 crystallite would be modified, and a large amount of Al_2O_3 would block proportionally few total adsorption sites.

The conclusion that, for equivalent amounts of surface oxidic material, titania exists in a more highly dispersed state than does alumina on a nickel surface may be related to raft formation in nickel particles supported on titania. Electron microscopy studies have suggested that high-temperature reduction can induce a spreading, or wetting, of three-dimensional hemispherical nickel crystallites to form thin crystallites, or "rafts" (*49, 51*). This behavior was first reported by workers at Exxon for titania-supported platinum (*52, 53*). Partial reduction of the support to Ti_4O_7 was thought to be a prerequisite to raft formation. Presumably, a strong driving force exists to maximize the titania-metal interfacial contact area, and thereby maximize support–metal bond formation.

As concluded by Santos *et al.* (*25*), the energetics of reduced titanium species spreading over Group VIII metals are similar to those of Group VIII metals spreading over reduced titania. Thus, due to the reducibility of transition-metal supports such as titania, reduced support species may exist as thin, highly dispersed entities on metallic surfaces, whereas irreducible supports such as alumina remain as large, discrete crystallites. This major structural difference is suggested to be a key reason why alumina-supported catalysts generally exhibit "weaker" metal–support interactions than corresponding titania-supported catalysts. A second reason may be related to the relative mobilities of oxide species from these supports, as discussed below.

In general, alumina-supported metals must be treated in hydrogen at temperatures 100–200 K higher than corresponding titania-supported metals to subsequently observe symptoms attributed to strong metal–support interactions (*37–39*). These temperatures are well above those normally employed in catalyst pretreatments and regeneration schemes. Thus, conventional supported materials like silica or alumina may not migrate for conditions under which

titania becomes mobile. This may be related to the reducibility of titania supports.

Overbury *et al.* (*54*) have reported that titania has a lower surface energy than silica or alumina. Addition of potassium to a Pt/TiO_2 catalyst has been shown to enhance the mobility of TiO_x moieties (*55*). Using Rutherford ion backscattering spectrometry (RIBS), Cairns *et al.* (*56*) investigated the diffusion of alumina and titania onto the surfaces of thin films of Rh or Pt. Both alumina and titania were found to diffuse onto the Pt metal surface, although alumina required a hydrogen treatment temperature 100 K higher than titania. Only titania diffused onto the Rh surface.

CONCLUSIONS

Study of the adsorption/desorption behavior of hydrogen and carbon monoxide on nickel surfaces containing varying concentrations of titania, from 0.1 to 0.7 monolayer equivalents, showed that the effects of titania are short-ranged and can largely be explained in geometric terms. Titania adspecies block CO adsortion at strongly bound sites (believed to be sites atop individual Ni atoms) and enhance adsorption at more weakly bound sites (believed to be hollow or bridging sites between Ni atoms). Importantly, CO adsorption on titania-containing nickel occurs at sites that would not normally be occupied on clean nickel due to strong CO–CO repulsions. The long-range electronic effects of titania were estimated to be limited to a 6-kJ $\cdot$ mol^{-1} decrease in CO adsorption strength at a coverage of 0.1 monolayer titania. Because the effects of titania are predominantly short-ranged, it appears that titania adspecies *must* be present on large Group VIII metal crystallites to explain the effects attributed to so-called strong metal–support interactions.

In contrast to CO adsorption, hydrogen adsorption is strengthened by the presence of titania adspecies. The relative shifts in CO and hydrogen adsorption strength should lead to more competitive hydrogen adsorption for titania-supported nickel catalysts under methanation conditions.

Alumina adspecies modify the chemisorptive properties of a nickel surface in a manner qualitatively similar to titania. An identical amount of titania altered nickel to a greater degree than alumina, suggesting that the titania exists in a more highly dispersed state on the Ni surface. Furthermore, since alumina may be less mobile than reduced titania, alumina moieties may not migrate onto the surfaces of alumina-supported Group VIII metal particles under conditions for which titania migrates in titania-supported catalysts. Nevertheless, the results of this study suggest that, given proper treatment conditions, the presence of metal oxide species on metal surface may be generalized to include not only reducible supports like titania but also irreducible supports like alumina.

ACKNOWLEDGMENTS

We gratefully acknowledge the financial support of a Kodak Graduate Fellowship for G.B.R. Financial support from the National Science Foundation was also received and is greatly appreciated.

REFERENCES

1. Raupp, G. B., and Dumesic, J. A., *J. Phys. Chem.* **88,** 660 (1984).
2. Kugler, E. L., and Garten, R. L. U.S. Patent No. 4,273,724, June 16, 1981.
3. Vannice, M. A., and Sudhakar, C., *J. Phys. Chem.* **88,** 2429 (1984).
4. Chung, Y.-W., Xiong, G., and Kao, C.-C., *J. Catal.* **85,** 237 (1984).
5. Raupp, G. B., Ph.D. thesis. University of Wisconsin, Madison, 1984.
6. Benziger, J. B., and Madix, R. J., *Surf. Sci.* **79,** 394 (1979).
7. McCarty, J. G., and Madix, R. J., *Surf. Sci.* **54,** 121 (1976).
8. Ko, E. I., and Madix, R. J., *Appl. Surf. Sci.* **3,** 236 (1979).
9. Falconer, J. L., and Madix, R. J., *Surf. Sci.* **48,** 393 (1975).
10. Ibach, H., Erley, W., and Wagner, H., *Surf. Sci.* **92,** 29 (1980).
11. Raupp, G. B., and Dumesic, J. A., accepted for publication in *J. Phys. Chem.*
12. Kiskinova, M., and Goodman, D. W., *Surf. Sci.* **108,** 64 (1981).

13. Madix, R. J., Thornburg, M., and Lee, S. B., *Surf. Sci.* **133,** L447 (1983).
14. Tracy, J. C., *J. Chem. Phys.* **56,** 2736 (1972).
15. Klier, K., Zettlemoyer, A. C., and Leidheiser, H., Jr., *J. Chem. Phys.* **52,** 589 (1970).
16. Kiskinova, M. P., *Surf. Sci.* **111,** 584 (1981).
17. Kiskinova, M., and Goodman, D. W., *Surf. Sci.* **105,** 1265 (1981).
18. Tomanek, D., and Bennemann, K. H., *Surf. Sci.* **127,** L111 (1983).
19. Johnson, S., and Madix, R. J., *Surf. Sci.* **108,** 77 (1981).
20. Gland, J. L., Madix, R. J., McCabe, R. W., and DeMaggio, C., *Surf. Sci.* **143,** 46 (1984).
21. Blyholder, G. B., *J. Phys. Chem.* **68,** 2772 (1964).
22. Blyholder, G. B., *J. Vac. Sci. Technol.* **11,** 865 (1974).
23. Muetterties, E. L., Rhodin, T. N., Band, E., Brucker, C. F., and Pretzer, W. R., *Chem. Rev.* **79,** 1 (1979).
24. Christmann, K., Ertl, G., and Schober, O., *Surf. Sci.* **40,** 61 (1975).
25. Santos, J., Phillips, J., and Dumesic, J. A., *J. Catal.* **81,** 147 (1983).
26. Anderson, S., *Solid State Commun.* **21,** 75 (1977).
27. Biberian, J. P., and Van Hove, M. A., *Surf. Sci.* **118,** 443 (1982).
28. Prichard, J., *Surf. Sci.* **79,** 231 (1979).
29. Takatani, S., and Chung, Y.-W., *J. Catal.* **90,** 75 (1984).
30. Campuzano, J. C., and Greenler, R. G., *Surf. Sci.* **83,** 301 (1979).
31. Germer, L. H., May, J. W., and Szostek, R. J., *Surf. Sci.* **7,** 403 (1967).
32. Holloway, P. H., and Hudson, J. B., *J. Vac. Sci. Technol.* **12,** 647 (1975).
33. Rhodin, T. N., and Demuth, J. E., *Jpn. J. Appl. Phys., Suppl. 2, Part 2,* 167 (1974).
34. Bartholomew, C. H., Pannel, R. B., and Butler, J. L., *J. Catal.* **63,** 335 (1980).
35. Vannice, M. A., and Twu, C. C., *J. Catal.* **82,** 213 (1983).
36. Ozdogan, S. C., Gochis, P. D., and Falconer, J. L., *J. Catal.* **83,** 257 (1983).
37. Menon, P. G. and Froment, G. F., *J. Catal.* **59,** 138 (1979).
38. Dautzenberg, F. M., and Wolters, H. B. M., *J. Catal.* **51,** 26 (1978).
39. den Otter, G. J., and Dautzenberg, F. M., *J. Catal.* **53,** 116 (1978).
40. Martin, G. A., Dutartre, R., and Dalmon, J. A., *React. Kinet. Catal. Lett.* **16,** 329 (1981).
41. Martin, G. A., and Dalmon, J. A., *React. Kinet. Catal. Lett.* **16,** 325 (1981).
42. Praliaud, H., and Martin, G. A., *J. Catal.* **72,** 394 (1981).
43. Beck, D. D., and White, J. M., *J. Phys. Chem.* **88,** 2764 (1984).
44. Beck, D. D., Banagan, A. O., and White, J. M., *J. Phys. Chem.* **88,** 2771 (1984).
45. Abbas, N. M., and Madix, R. J., *Surf. Sci.* **62,** 739 (1977).
46. Madix, R. J., *Catal. Rev. Sci. Eng.* **15**(2), 293 (1977).
47. Ying, D. H. S., and Madix, R. J., *J. Inorg. Chem.* **17,** 1103 (1978).
48. Apple, T. M., Gajardo, P., and Dybowski, C., *J. Catal.* **68,** 103 (1981).
49. Simoens, A. J., Baker, R. T. K., Dwyer, D. J., Lund, C. R. F., and Madon, R. J., *J. Catal.* **86,** 359 (1984).
50. Gorte, R. J., *Amer. Chem. Soc., Div. Pet. Chem. Prepr.* **30,** 143 (1985).
51. Smith, J. S., Thrower, P. A., and Vannice, M. A., *J. Catal.* **68,** 270 (1981).
52. Baker, R. T. K., Prestridge, E. B., and Garten, R. L., *J. Catal.* **56,** 390 (1979).
53. Baker, R. T. K., Prestridge, E. B., and Garten, R. L., *J. Catal.* **59,** 293 (1979).
54. Overbury, S. H., Bertrand, P. A., and Somorjai, G. A., *Chem. Rev.* **75,** 547 (1975).
55. Spencer, M. S., *J. Phys. Chem.* **88,** 1046 (1984).
56. Cairns, J. A., Baglin, J. E. E., Clark, G. J., and Ziegler, J. F., *J. Catal.* **83,** 301 (1983).